electronics

MDPI

Communication

Beneficial Effects of Self-Motion for the Continuous Phase Analysis of Ac-Coupled Doppler Radars

Luigi Ferro [1,*], Changzhi Li [2], Graziella Scandurra [1], Carmine Ciofi [1] and Emanuele Cardillo [1]

[1] Department of Engineering, University of Messina, 98166 Messina, Italy; gscandurra@unime.it (G.S.); cciofi@unime.it (C.C.); ecardillo@unime.it (E.C.)
[2] Department of Electrical and Computer Engineering, Texas Tech University, Lubbock, TX 79409, USA; changzhi.li@ttu.edu
* Correspondence: luferro@unime.it

Abstract: This paper analyzes the beneficial effects on phase detection arising from the motion of an ac-coupled Doppler radar. Indeed, although the presence of an ac coupling stage suppresses the dc offset after the receiver RF output, due to the coupling capacitor, a high-pass behavior is introduced; the presence of a high-pass behavior leads to signal distortion, particularly for low Doppler frequencies, which are typical in many biomedical or industrial applications. Since the target displacement is usually extracted from the phase history, this effect might, in turn, worsen the overall accuracy of the system. Moreover, if the target alternates stationary and moving time intervals, the phase detection step becomes challenging. Indeed, during the stationary time, the output of the RF front-end shows only noise fluctuations that, in turn, result in uncorrelated phases which might be confused with the real target displacement. This negative effect might be avoided by keeping the radar continuously moving, thus exploiting what is usually considered a state that is negative and worthy of attention. In this contribution, this effect is addressed from a different perspective, and ad hoc experimental case studies are shown to demonstrate the effectiveness of the proposed system. This task has been accomplished through theoretical analysis and related experimental activity.

Keywords: ac-coupling; Doppler radar; low-frequency noise; phase analysis; radar self-motion

check for updates

Citation: Ferro, L.; Li, C.; Scandurra, G.; Ciofi, C.; Cardillo, E. Beneficial Effects of Self-Motion for the Continuous Phase Analysis of Ac-Coupled Doppler Radars. *Electronics* **2024**, *13*, 772. https://doi.org/10.3390/electronics13040772

Academic Editor: Yide Wang

Received: 15 December 2023
Revised: 6 February 2024
Accepted: 14 February 2024
Published: 16 February 2024

Copyright: © 2024 by the authors. Licensee MDPI, Basel, Switzerland. This article is an open access article distributed under the terms and conditions of the Creative Commons Attribution (CC BY) license (https://creativecommons.org/licenses/by/4.0/).

1. Introduction

Most microwave Doppler radars exploit a homodyne architecture with the task of measuring the target phase history and to obtain information concerning the related target displacement [1–8]. Although direct conversion receivers have demonstrated their effectiveness and reduced phase noise, their performance is seriously affected by the ever-present dc offset in the baseband section. As an example, the presence of dc offset might reduce the dynamic range of the receiver by saturating the amplifiers in the baseband stage [9–11]. In conventional continuous wave CW radars, the dc offset might occur mainly for a twofold undesired reason: hardware imperfections and clutter presence [12,13]. The former can be due to component mismatch, poor isolation and the related mixing between the microwave signal and the local–oscillator (LO) path, either through the antennas or from substrate coupling. The latter is due to the signals reflected by the stationary parts of the target of interest or by additional stationary objects in the background.

Since the dc component can be several orders of magnitude larger than the amplitude of the signal of interest, e.g., the low-level baseband signal related to the respiratory or heart activity, it makes the extraction of the desired information with reasonable resolution very challenging [14–17].

To remove the dc-offset directly, i.e., without implementing post-processing dc-offset compensation techniques, many researchers and radar suppliers propose ac-coupled receivers whereby a high-pass filter removes the dc content. Although the filtering section

is usually designed with the purpose of obtaining a cut-off frequency as low as possible to preserve the signal content, this is often not the case. In conventional radars, signal distortion is introduced, particularly when the target motion has low Doppler frequency components [1,18,19].

Moreover, if the target of interest alternates stationary and moving periods, the low-frequency output of the RF front-end during the stationary time shows only noise fluctuations, which in turn result in uncorrelated phases. This will lead to a wrong measured phase history and consequently to a challenging detection of the desired target displacement [20].

Since the radar measures relative movements, regardless of whether the target or the radar itself is moving, this negative effect might be avoided by keeping the radar continuously moving. Indeed, in this case, the mixing between the LO and the received signal will be always different from zero, except for the unlikely case of a target having exactly the same speed as the radar. In the scientific literature, the radar motion is often considered a negative state, e.g., for the task of vital sign detection while the radar is mounted on a moving platform, as an unmanned aerial vehicle [21,22]. Indeed, when the radar moves, the relative range detection is often many orders of magnitude larger than the desired signal and needs to be corrected. This often requires implementing techniques to obtain the movement of the radar itself which in turn can be subtracted from measured data [23].

On the other hand, a small number of works deal with intentionally leveraging the radar movement [24,25]. As an example, in [24], the authors take advantage of the radar movement to find the target direction with a single-input single-output Doppler radar. To clarify, the induced Doppler shift involves different Doppler returns from echoes at different angles, which can, in turn, be exploited to obtain angle detection capabilities with small aperture antennas.

In this paper, the effect of the radar motion during the measurement of small displacements is investigated. To this purpose, a millimeter-wave radar is intentionally moved by means of a controlled mini-actuator, while measuring the target displacement.

During the experimental activity, the stationary and movement periods of the radar have been alternated to highlight the issue arising from the uncorrelated phase histories during the stationary periods and how the detection can be effectively and successfully achieved during the movement periods. This contribution can be useful for those researchers interested in continuous monitoring via ac-coupled radars of targets alternating moving and stationary periods, both to further investigate the issue and to enhance detection if a moving radar platform is available. Indeed, when the radar moves, the noisy zero-Doppler outputs are suppressed and thus the random phase histories are too.

In Section 2, a theoretical description of the main working principle required to enhance the phase detection with ac-coupled Doppler radars is provided, whereas the experimental characterization of the scenario is reported in Section 3. The conclusive remarks are finally drawn in Section 4.

2. Analysis of Target Detection with Moving Radar

Figure 1 shows the typical architecture of an ac-coupled quadrature Doppler radar. If the demodulated in-phase $s_I(t)$ and quadrature $s_Q(t)$ (IQ) signals are far enough from the filter cutoff frequency, they can be written as shown in (1) and (2).

$$s_I(t) = \sigma_R \cos\left(\Delta\phi \pm \frac{4\pi x(t)}{\lambda}\right), \tag{1}$$

$$s_Q(t) = \sigma_R \sin\left(\Delta\phi \pm \frac{4\pi x(t)}{\lambda}\right), \tag{2}$$

where σ_R is the amplitude of the down-converted signal, $\Delta\phi$ is the residual phase, λ is the wavelength and $x(t)$ is the target displacement.

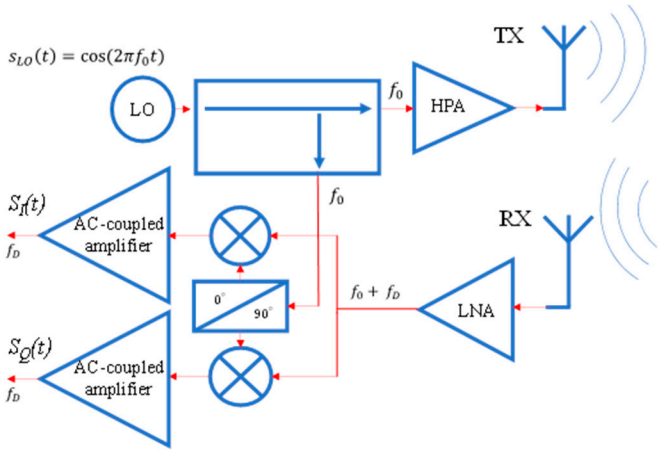


Figure 1. Block diagram of a continuous-wave ac-coupled radar system with quadrature mixer.

When the target is stationary, the null-Doppler shift will result in a dc level at the outputs of the mixer. The ac-coupling stage behaves as a high-pass filter, thus cutting the dc level together with the lower portion of the frequency spectrum. During the stationary period, the presence of noise fluctuations after the ac-coupling stage will generate uncorrelated phases, which in turn will result in wrong displacement estimation.

This concept might be better explained by observing the IQ signals shown in Figure 2. Figure 2a shows a target with nonzero velocity from 2.2 s to 3.2 s. This is evident by observing the related higher dynamic of the signal which suggests the presence of a moving target in the scenario. However, since after the phase extraction step, the information concerning the signal amplitude is lost, and it is no longer possible to separate movement and stationary times and, consequently, correct random displacements. The constellation graphs, reported in Figure 2b,c, highlight this concept. Indeed, although both graphs show a rotating complex signal, only the phasor reported in Figure 2b, which is extracted during a 10 ms motion time, includes a correct phase. The phasor shown in Figure 2c, which is extracted during 10 ms of stationary time, exhibits an uncorrelated phase.

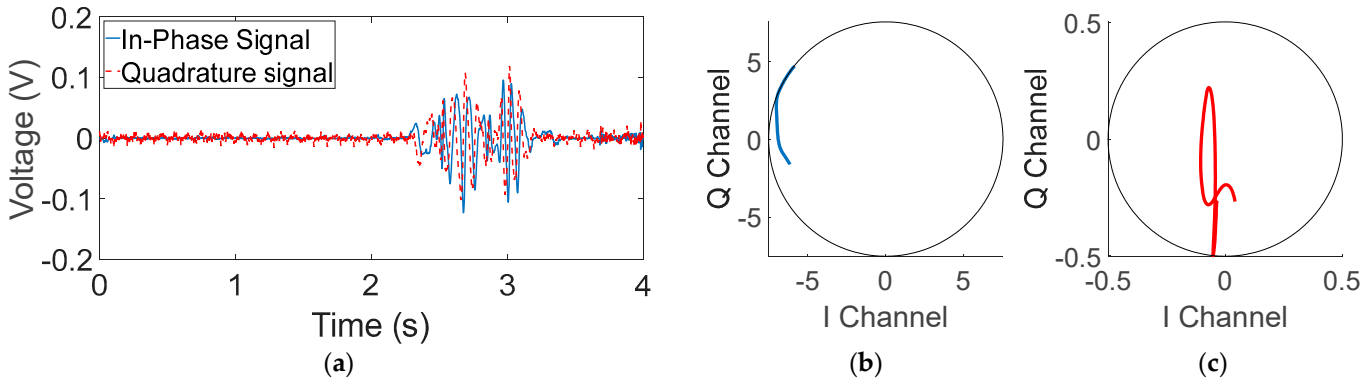


Figure 2. (**a**) In−Phase (blue solid line) and Quadrature (red dotted line) signals vs. time. IQ signals in a constellation graph during 10 ms of (**b**) motion time and (**c**) stationary time.

The effect on the phase history can be observed in Figure 3, from which the phase history resulting from the stationary or movement periods cannot be separated. As a consequence, the stationary time leads to wrong evaluations that not only make the correct measured phase during target motion periods unrecognizable but modifies also the initial phase of the target motion periods, shifting the entire level of the displacement.

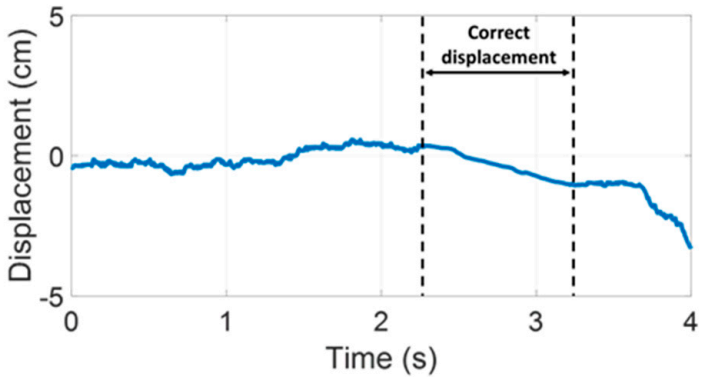


Figure 3. Measured displacement. The target moving time is from 2.2 s to 3.2 s.

When the target is moving, i.e., between 2.2 s and 3.2 s, the displacement would be properly detected, e.g., by applying the arctangent demodulation [26,27].

Based on these considerations, it is worth noting that if the radar is instead moving during the measurement, the expressions of the IQ signals change as reported in (3) and (4).

$$s_I(t)' = \sigma_R \cos\left(\Delta\phi \pm \frac{4\pi x(t)}{\lambda} \pm \frac{4\pi\, r(t)}{\lambda}\right), \tag{3}$$

$$s_Q(t)' = \sigma_R \sin\left(\Delta\phi \pm \frac{4\pi x(t)}{\lambda} \pm \frac{4\pi\, r(t)}{\lambda}\right), \tag{4}$$

where $r(t)$ is the displacement introduced by to the continuous radar motion.

The presence of the term $r(t)$ imposes an ever-present signal at the output of the mixers, involving correct measured phase histories. Of course, the radar motion affects the displacement detection by adding an additional apparent target movement that needs to be corrected.

3. Continuous Phase History Detection

The system has been tested with the experimental setup shown in the picture in Figure 4.

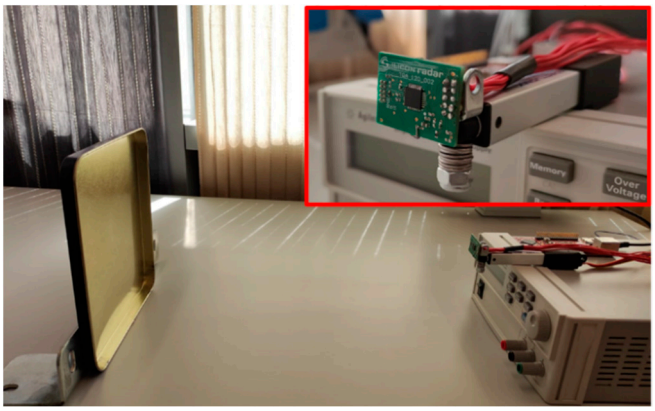


Figure 4. Picture of the experimental setup.

In detail, a 120 GHz radar based on the TRA_120_002 by Indie Semiconductor has been mounted on an actuator moving at a constant speed of 10 mm/s for a total measurement time of 5 s [28]. The millimeter-wave radar, mounted on the moving actuator, is shown on the right side of Figure 4. The TRA_120_002 is an integrated chip including both the transceiver and the transmitting and receiving antennas. The presence of antennas-on-chip allows us to impressively reduce the dimension of the radar. The front-end board is connected to an analog-to-digital conversion board which collects the data and sends it

out to a laptop for the relative signal elaboration. The small dimensions of the radar, due to the high working frequency, are very beneficial for reducing the weight of the system, thus minimizing possible unwanted vibrations during the motion periods. The target is a 20 cm × 20 cm metallic plate, shown on the left side of Figure 4.

Due to the presence of the wavelength in Equations (1)–(4), it is worth analyzing the performance dependance on the frequency stability. The output frequency of the TRA_120_002 can be controlled by four voltage-controlled oscillator (VCO) tuning inputs. The stability of the chip output frequency deserves considerations based on its dependance on the supply voltage and temperature. The dependance on the supply voltage can be neglected. Indeed, the supply voltage is the output of a stable voltage regulator, and the chip exhibits an average output frequency shift lower than 100 MHz for a 0.3 V voltage drift, which is of course an overestimate value for a voltage regulator.

On the other hand, the dependance on the temperature is usually considered a critical factor for the stability of the output frequency. The chip exhibits a 1 GHz average output frequency shift for quite a wide temperature range, i.e., from 10 °C to 90 °C. However, although the output frequency dependance on the temperature seriously affects the performance of FMCW radars, it can be also considered negligible in this scenario [29–34]. Indeed, by considering a target moving at the maximum unambiguous speed, the phase change across the measurement is π, i.e., a $\frac{\lambda}{4}$ displacement change. According to the component's datasheet, the frequency shift is around 15 MHz for each 1 °C of temperature drift. As an example, by considering an excessively negative scenario, i.e., 1 °C temperature drift for each second, since the data are acquired each 10 ms, the frequency shift will be approximately 150 kHz for each measurement.

As a consequence, the wavelength shift will be approximately 3 nm for each measurement and the resulting error on the displacement will be approximately 0.76 nm for each measurement, which is a negligible value in this context.

The controlled radar movement is measured from the echo of a stationary target and subtracted from the next measurements, thus removing the effect of the radar motion on the displacement and correcting the desired data. Figure 5a shows two different measurements, both performed on a stationary target, to test the effectiveness and the repeatability of the procedure. According to the previous analysis, since the radar is moving for the first 5 s and, later, it is instead stationary during the next 3 s, different results on the phase extraction are expected.

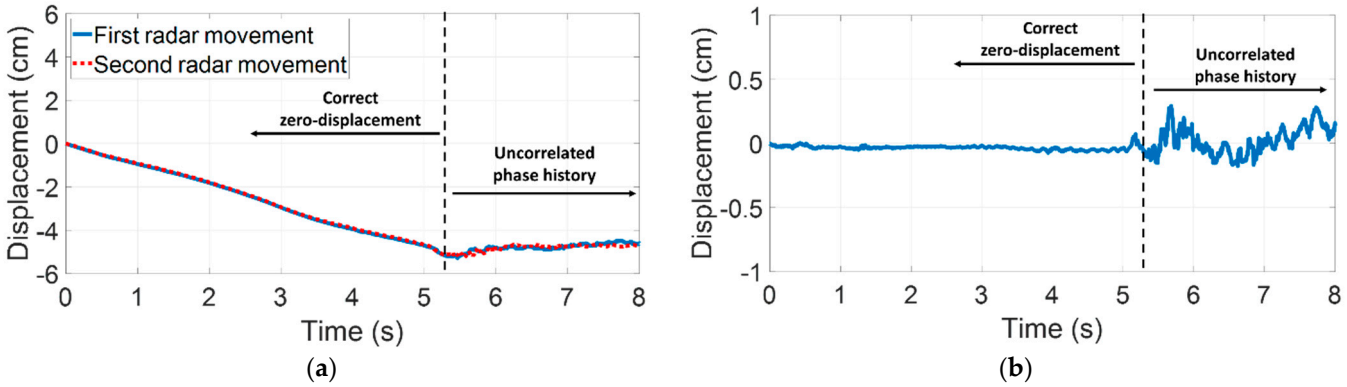


Figure 5. (**a**) First (blue solid line) and second (red dotted line) displacement from a stationary target and (**b**) difference between the two measurements.

To clarify, during the radar movement, i.e., up to 5.2 s, the correct zero-displacement can be extracted after the removal step, i.e., after removing the displacement due to the radar motion itself. When the radar is also stationary, i.e., from 5.2 s, both measurements show random and uncorrelated phase histories that in turn result in the wrong displacement detection of the last part of Figure 5b.

Thereafter, the system has been tested to detect a moving target, i.e., a metallic plate moving 1.2 cm back and forth. Due to the continuous radar motion throughout the entire measurement, a down-converted signal is always present and the phase history extraction with the arctangent demodulation always makes sense. This can be noticed from Figure 6, where the radar moves during the entire measurement and, after removing the effect of the radar motion from the data, the desired results are obtained. The maximum distance covered by the plate is highlighted by means of markers in Figure 6.

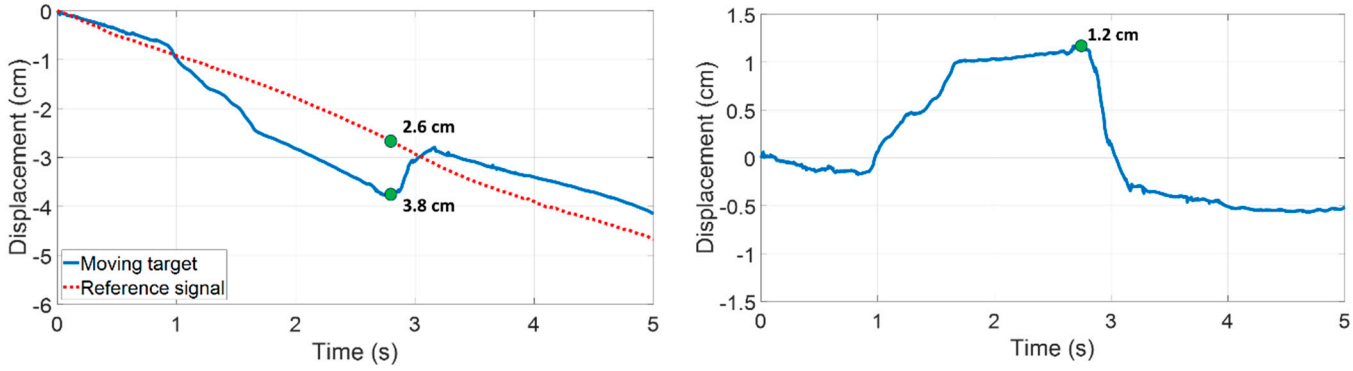


Figure 6. (**a**) Refence signal (red dotted line) and measured displacements from an alternating moving target (blue solid line) and (**b**) difference between the two measurements.

It should be observed that, since imposing mechanical movements can be expensive or impractical to produce in some environments, modifying the radar signal to digitally create an effect similar to a real radar movement might represent a more efficient way to solve the issue. As an example, for a constant-velocity linear motion, a possible solution might consist of applying a frequency offset between the transmitted and the LO signals, that, in turn, will result in a fixed tone after the mixer. The related absence of noise fluctuations after the ac-coupling stage will avoid the occurrence of uncorrelated phases, whereas the correct phase can be again obtained after subtracting the phase corresponding to the artificial tone from the measured phase.

4. Conclusions

In this paper, the intentional radar motion is exploited to extract the real target displacement. Indeed, a noisy contribution is usually present at the output of the receiver for ac-coupled Doppler radars while echoes from stationary targets are received. This leads to wrong displacement detections which are difficult to correct. This negative effect is suppressed by keeping the radar continuously moving, thus positively exploiting what is usually considered a negative condition. This work can be useful for those researchers interested in the continuous monitoring of targets with ac-coupled radars, both to further investigate the issue and to enhance the detection.

Author Contributions: Conceptualization, L.F. and E.C.; methodology, L.F. and E.C.; software, L.F. and E.C.; validation, L.F. and E.C.; formal analysis, L.F. and E.C.; investigation, L.F., C.L., G.S., C.C. and E.C.; resources, L.F. and E.C.; data curation, L.F. and E.C.; writing—review and editing, L.F., C.L., G.S., C.C. and E.C. All authors have read and agreed to the published version of the manuscript.

Funding: This research received no external funding.

Data Availability Statement: Data are contained within the article.

Conflicts of Interest: The authors declare no conflicts of interest.

References

1. Yavari, E.; Lubecke, V.; Borić-Lubecke, O. Ac/dc coupling effects on CW and pulse transmission modes in Doppler radar physiological monitoring system. In Proceedings of the 2012 IEEE Topical Conference on Biomedical Wireless Technologies, Networks, and Sensing Systems (BioWireleSS), Santa Clara, CA, USA, 15–18 January 2012; pp. 25–28. [CrossRef]
2. Droitcour, A.D.; Borić-Lubecke, O.; Lubecke, V.M.; Lin, J.; Kovacs, G.T.A. Range correlation and I/Q performance benefits in single-chip silicon Doppler radars for noncontact cardiopulmonary monitoring. *IEEE Trans. Microw. Theory Tech.* **2004**, *52*, 838–848. [CrossRef]
3. Vergara, A.M.; Borić-Lubecke, O.; Lubecke, V.M. Dc information preservation for cardiopulmonary monitor utilizing CW doppler radar. In Proceedings of the 2008 30th Annual International Conference of the IEEE Engineering in Medicine and Biology Society, Vancouver, BC, Canada, 20–25 August 2008; pp. 1246–1249. [CrossRef]
4. Cardillo, E.; Sapienza, G.; Ferro, L.; Li, C.; Caddemi, A. Radar assistive system for people with neurodegenerative disorders through head motion and eyes blinking detection. In Proceedings of the International Microwave Symposium (IMS), San Diego, CA, USA, 11–16 June 2023. [CrossRef]
5. Cardillo, E.; Ferro, L.; Li, C. Microwave and millimeter-wave radar circuits for the next generation contact-less in-cabin detection. In Proceedings of the Asia-Pacific Microwave Conference APMC'22, Yokohama, Japan, 29 November–2 December 2022; pp. 231–233. [CrossRef]
6. Cardillo, E.; Ferro, L.; Sapienza, G.; Li, C. Reliable eye-blinking detection with millimeter-wave radar glasses. *IEEE Trans. Microw. Theory Tech.* **2024**, *72*, 771–779. [CrossRef]
7. Dahlbäck, R.; Bryllert, T.; Granström, G.; Ferndahl, M.; Drakinskiy, V.; Stake, J. Compact 340 GHz homodyne transceiver modules for FMWC imaging radar arrays. In Proceedings of the 2016 IEEE MTT-S International Microwave Symposium (IMS), San Francisco, CA, USA, 22–27 May 2016; pp. 1–4. [CrossRef]
8. Arab, H.; Dufour, S.; Moldovan, E.; Akyel, C.; Tatu, S.O. A 77-GHz six-port sensor for accurate near-field displacement and Doppler measurements. *Sensors* **2018**, *18*, 2565. [CrossRef] [PubMed]
9. Obradović, D.V.; Glavonjić, Đ.P.; Krčum, D.P.; Mihajlović, V.R.; Milosavljević, I.M. A highly programmable 60-dB gain analog baseband circuit with DC-offset cancellation for short-range FMCW radar applications. *Analog Integr. Circ. Sig. Process* **2020**, *104*, 299–309. [CrossRef]
10. Wu, W.; Zhang, L.; Wang, Y. A PVT-robust analog baseband with DC offset cancellation for FMCW automotive radar. *IEEE Access* **2019**, *7*, 43249–43257. [CrossRef]
11. Lee, I.-S.; Park, J.-H.; Yang, J.-R. Detrending technique for denoising in CW radar. *Sensors* **2021**, *21*, 6376. [CrossRef] [PubMed]
12. Juan, P.-H.; Chen, K.-H.; Wang, F.-K. Frequency-offset self-injection-locked radar with digital frequency demodulation for SNR improvement, elimination of EMI issue, and DC offset calibration. *IEEE Trans. Microw. Theory Tech.* **2021**, *69*, 1149–1160. [CrossRef]
13. Michler, F.; Schoenhaerl, S.; Schellenberger, S.; Shi, K.; Scheiner, B.; Lurz, F.; Weigel, R.; Koelpin, A. An automatic gain and offset control circuit for DC-coupled continuous-wave radar systems. In Proceedings of the 2020 IEEE/MTT-S International Microwave Symposium (IMS), Los Angeles, CA, USA, 4–6 August 2020; pp. 980–983. [CrossRef]
14. Park, B.-K.; Boric-Lubecke, O.; Lubecke, V.M. Arctangent demodulation with DC offset compensation in quadrature Doppler radar receiver systems. *IEEE Trans. Microw. Theory Tech.* **2007**, *55*, 1073–1079. [CrossRef]
15. Kontou, P.; Smida, S.B.; Dragone, M.; Nikolaou, S.; Anagnostou, D.E. CW radar based system with automated DC offset reduction for heartbeat detection. In Proceedings of the 2020 IEEE USNC-CNC-URSI North American Radio Science Meeting (Joint with AP-S Symposium), Montreal, QC, Canada, 5–10 July 2020; pp. 73–74. [CrossRef]
16. Kim, Y.J.; Kim, D.K. Experimental characterization process of DC-offset performance for multiple CW Doppler radar. In Proceedings of the 2019 34th International Technical Conference on Circuits/Systems, Computers and Communications (ITC-CSCC), JeJu, Republic of Korea, 23–26 June 2019; pp. 1–3. [CrossRef]
17. Yang, Z.-P.; Chiang, Y.-C. Vital signal radar with adaptive compensation circuits to effectively eliminate DC Offsets. *IEEE Microw. Wirel. Compon. Lett.* **2018**, *28*, 88–90. [CrossRef]
18. Lubecke, V.; Borić-Lubecke, O.; Ishrak, M.S.; Wu, T.; Cai, F. Radar Monitoring in Sleep Medicine. In Proceedings of the 16th International Conference on Advanced Technologies, Systems and Services in Telecommunications (TELSIKS), Nis, Serbia, 25–27 October 2023; pp. 109–113. [CrossRef]
19. Gu, C.; Li, R.; Zhang, H.; Fung, A.Y.; Torres, C.; Jiang, S.B.; Li, C. Accurate respiration measurement using dc-coupled continuous-wave radar sensor for motion-adaptive cancer radiotherapy. *IEEE Trans. Biomed. Eng.* **2012**, *59*, 3117–3123. [CrossRef] [PubMed]
20. Ferro, L.; Scandurra, G.; Li, C.; Cardillo, E. Robust Doppler displacement measurement resolving the uncertainty during target stationary moment. In Proceedings of the IEEE Radio & Wireless Week (RWW2024), San Antonio, TX, USA, 21–24 January 2024; pp. 57–60.
21. Islam, S.M.M.; Oba, L.; Lubecke, V.M. Empirical Mode Decomposition (EMD) for platform motion compensation in remote life sensing radar. In Proceedings of the 2022 IEEE Radio and Wireless Symposium (RWS), Las Vegas, NV, USA, 16–19 January 2022; pp. 41–44. [CrossRef]
22. Islam, S.M.M.; Lubecke, L.C.; Grado, C.; Lubecke, V.M. An adaptive filter technique for platform motion compensation in unmanned aerial vehicle based remote life sensing radar. In Proceedings of the 2020 50th European Microwave Conference (EuMC), Utrecht, Netherlands, 12–14 January 2021; pp. 937–940. [CrossRef]

23. Cardillo, E.; Li, C.; Caddemi, A. Vital sign detection and radar self-motion cancellation through clutter identification. *IEEE Trans. Microw. Theory Tech.* **2021**, *69*, 1932–1942. [CrossRef]
24. Chordas-Ewell, N.; Xu, K.; Kadlimatti, R.; Fam, A.T.; Choi, J.H. Vibrating antenna Doppler radar. In Proceedings of the 17th European Radar Conference (EuRAD), Utrecht, Netherlands, 10–15 January 2021; pp. 242–245. [CrossRef]
25. Liu, J.; Zhang, Y.D.; Amin, M.G. Target localization in moving radar platform exploiting range and Doppler information through semidefinite relaxation. In Proceedings of the Wireless Sensing, Localization, and Processing V SPIE 7706, Orlando, FL, USA, 28 April 2010. [CrossRef]
26. Li, J.; Chen, Y.; Yao, S.; Li, P.; Yin, K.; Wu, Q. Harmonic suppression phase gradient demodulation for vital sign monitoring. *IEEE Trans. Instrum. Meas.* **2024**, *73*, 4000716. [CrossRef]
27. Sameera, J.N.; Ishrak, M.S.; Lubecke, V.M.; Boric-Lubecke, O. Enhancing beat-to-beat analysis of heart signals with respiration harmonics reduction through demodulation and template matching. *IEEE Trans. Microw. Theory Tech.* **2024**, *72*, 750–758. [CrossRef]
28. Indie Semiconductor; Silicon Radar GmBH. *Datasheet_TRA_120_002 120-GHz Highly Integrated IQ Transceiver with Antennas on Chip in Silicon Germanium Technology*, Revision 0.8; Silicon Radar GmBH: Frankfurt, Germany, 2018.
29. Zhou, M.; Liu, Y.; Wu, S.; Wang, C.; Chen, Z.; Li, H. A novel scheme of high-precision heart rate detection with a mm-wave FMCW radar. *IEEE Access* **2023**, *11*, 85118–85136. [CrossRef]
30. Yang, M.; Chen, J.; Shan, C. Phase locked-loop design of high-order automotive frequency modulated continuous wave radar based on fast integration structure. *IEEE Access* **2024**, *12*, 11926–11935. [CrossRef]
31. Hadidian, B.; Khoeini, F.; Hossein Naghavi, S.M.; Cathelin, A.; Sarabandi, K.; Afshari, E. A 194-238 GHz fully on-chip self-referenced frequency stabilized radiator for high range resolution imaging. In Proceedings of the 2023 IEEE Custom Integrated Circuits Conference (CICC), San Antonio, TX, USA, 23–26 April 2023; pp. 1–2. [CrossRef]
32. Arai, T.; Usugi, T.; Murakami, T.; Kishimoto, S.; Utagawa, Y.; Kohtani, M.; Arai, C.; Arai, T.; Yamaura, S. A 77-GHz 8RX3TX transceiver for 250-m long-range automotive radar in 40-nm CMOS technology. *IEEE J. Solid-State Circuits* **2021**, *56*, 1332–1344. [CrossRef]
33. Wu, J.; Deng, W.; Chen, Z.; Zheng, W.; Liu, Y.; Wang, S.; Qi, N.; Chi, B. A 77-GHz mixed-mode FMCW generator based on a vernier TDC with dual rising-edge fractional-phase detector. *IEEE Trans. Circuits Syst. I Regul. Pap.* **2020**, *67*, 60–73. [CrossRef]
34. Shen, Z.; Li, H.; Jiang, H.; Zhang, Z.; Liu, J.; Liao, H. A 12-GHz all-digital calibration-free FMCW signal generator based on a retiming fractional frequency divider. In Proceedings of the 2019 IEEE Asian Solid-State Circuits Conference (A-SSCC), Macau, 4–6 November 2019; pp. 287–290. [CrossRef]

Disclaimer/Publisher's Note: The statements, opinions and data contained in all publications are solely those of the individual author(s) and contributor(s) and not of MDPI and/or the editor(s). MDPI and/or the editor(s) disclaim responsibility for any injury to people or property resulting from any ideas, methods, instructions or products referred to in the content.